Journal of Sound and Vibration (2000) **234**(4), 555–576
doi:10.1006/jsvi.1999.2752, available online at http://www.idealibrary.com on IDEAL®

A WAVELET-BASED APPROACH FOR THE IDENTIFICATION OF LINEAR TIME-VARYING DYNAMICAL SYSTEMS

ROGER GHANEM

The Johns Hopkins University, Baltimore, MD 21218, *U.S.A.*

AND

FRANCESCO ROMEO

Università di Roma "La Sapienza", Rome, Italy

(*Received* 27 *May* 1999, *and in final form* 21 *October* 1999)

A novel procedure is developed for the identification of linear discrete models of dynamical systems from noisy data. Of particular interest is the application of the methodology to time-varying systems. The procedure is based on a representation of the governing differential equations with respect to a wavelet basis, and the formulation of an inverse algebraic problem in the associated subspace. The effect of noisy data is considered and numerical simulations demonstrating the applicability of the method to single- and multi-degree-of-freedom dynamical systems are presented.

1. INTRODUCTION

Time-invariant (LTI) models are usually appropriate for describing the dynamical behavior of most structural systems under service loading. Under certain circumstances, however, the loading conditions are such that either the structure incurs significant damage, consequently changing its dynamical and mechanical parameters, or the magnitude of the loads is such that geometrically non-linear behaviour is excited. Moreover, structural systems accumulate damage under both service load and environmental excitations. In such cases, a linear time-varying (LTV) model may better capture the transition in the mode of operation of the system, and could be used to assess the condition of the system or to diagnose its failure. It is generally recognized that damage can be associated with a modification of the dynamical characteristics of the system, such as stiffness and damping [1]. As far as civil structures are concerned, it has been observed that a degradation of the stiffness of up to 70% can occur in either reinforced concrete or steel frames during strong earthquakes [2,3]. Besides confirming changes in natural frequencies of the structures between pre-earthquake and post-earthquake vibration tests, the above studies presented a detailed study of the response of two buildings adopting a moving window short-time Fourier transform (STFT) analysis. From this analysis emerged that changes to the dynamical and structural characteristics can be significantly larger than the reductions inferred from post-earthquake vibration tests and that these changes are strongly time-dependent. In order to improve the quasi-time-invariant linear formulation of the STFT, it was later proposed [4] to model the building structure as a

0022-460X/00/290555 + 22 $35.00/0

single-degree-of-freedom (s.d.o.f.) time-varying system the parameters of which were tracked in time through a Kalman Filter utilizing records of ground motion and structural accelerations. It was found that the ratio of the time-dependent natural frequency to the original value was a smooth time-varying function, which dropped to about half of its original value during the strong motion part of the excitation. Having considered that structures under strong environmental loads may undergo non-linear and time-dependent degrading behaviour, a real-time-domain technique was later proposed [1] to identify the time-varying system parameters for a multi-d.o.f degrading system. In this work the system parameters was assumed to be an arbitrary function of time and a least-squares method was employed to estimate the system parameters at every time instant based on input data and the corresponding response measurement. In a different context, time-dependent parameters were also used to model the dynamics of a semiactive bridge vibration absorber [5]. This time dependency of the parameter matrices was associated with the dynamic coupling between the vehicle suspension and the bridge structure. LTV systems have also been frequently used to model systems that have non-stationary properties.

A number of authors have recently addressed the identification problem by means of the theory of wavelets. The general trend has been to interpret the wavelet transform (WT) as a windowing technique characterized by a flexible time-frequency window. The evolution of the system is deduced from the wavelet transform of the response of the system. For instance, the fatigue damage of a structure has been modelled as a random impulse in the input signal [7], and the identification of occurrence time of these impulses have been investigated by taking the WT of the output signal. Such a detection is shown to be obtainable for appropriate choices of wavelets belonging to the Daubechies family. The WT adopting the wavelet of Morlet (a Gaussian-enveloped oscillating function) has been used [8] to represent the transients generated by faults in a helicopter gearbox. The use of the continuous wavelet transform has also been applied [9,10] to fault detection in a spur gear. An application of wavelets in space domain for crack identification in structural elements has also been presented [11]. In that study, the response of a cracked beam at a given time was first determined using a discrete integration method and then expressed in terms of a discrete wavelet series; abrupt changes of the coefficients in that expansion were shown to give an indication of the crack location. In reference [12] the amplitude of the wavelet coefficient of the spatially varying static solution of a one-dimensional (1-D) truss was used as a reference level for the regularity of the solution itself. The coefficients of the wavelet transform from the response of the damaged structure were then compared against this reference level, with significant discrepancies interpreted as indicative of damage locations. All the above-mentioned approaches for structural applications are not exempt of a number of drawbacks. For data with spatial extent, for example, the availability of signals such as displacements or strains throughout the analyzed structure does not seem to be a realistic requirement. Similarly, if the analysis refers to temporal data, it is not evident how to derive meaningful physical interpretations from the detected singularities expressed in terms of Fourier coefficients. In spite of such limitations, it is important to point out that the above investigations, demonstrate a growing attention toward the potential of the wavelet transform for analyzing non-stationary systems and detecting structural faults. Only for the case of linear time-invariant systems has the wavelet transform of the impulse response been effectively used to derive the estimation of modal parameters [13]. No other attempts have been made to develop a framework for parameter estimation using wavelets as the analyzing signals. The WT has also been used to enhance the quality of the estimates of the impulse response functions that have traditionally been evaluated using the inverse Fourier transform [14]. This step plays a key role in many structural identification techniques where physical modes, mode shapes and damping properties are derived from the

estimation of the eigenvalues and the associated eigenvectors. The analysis, however, was restricted to the estimation of time-invariant models. A wavelet-based identification procedure for the analysis of linear time-varying systems is presented in this paper. The study focuses on the identification of the parameters characterizing discrete mechanical systems modelled by ordinary differential equations. Such models are formulated in terms of lumped mass, damping and stiffness matrices and the analysis is based on measured time domain input/output data. The core of the identification algorithm consists of the estimation of the parameters associated with a differential equation model relating input and the output measurements which has been discretized following a Galerkin procedure using wavelet based [15,16]. In the next section, the identification technique for s.d.o.f. and 2-d.o.f. systems is presented for both linear time-invariant and linear time-varying systems. Following that, the performance of the proposed identification procedure in the presence of noisy data is discussed. Several pertinent numerical simulations are presented in the last section where systems featuring smooth, abrupt and periodic time variation of their parameters are studied.

2. IDENTIFICATION TECHNIQUE

The technique proposed in this paper consists of projecting the governing differential equation on a subspace spanned by a finite number of wavelets. The resulting algebraic equations are then rewritten with the parameters of the dynamical system as unknowns. A number of techniques are then presented for estimating the values of these parameters from input and output noisy data. The next subsection presents the methodology for s.d.o.f. systems which is then extended, in the following sections, to the analysis to multi-d.o.f. systems.

2.1. SINGLE-DEGREE-OF-FREEDOM SYSTEMS

In this subsection the Galerkin approach is used to discretize the ordinary differential equation of a s.d.o.f. subjected to a general excitation $f(t)$. The governing equation of motion is given by

$$m(t)\ddot{x}(t) + c(t)\dot{x}(t) + k(t)x(t) = f(t). \tag{1}$$

The parameters $m(t)$, $c(t)$ and $k(t)$ refer, respectively, to the time-varying mass, damping and stiffness of the system. The problem is next recast in the subspace spanned by the basis defined by the compactly supported Daubechies scaling functions given by $\varphi_{j,k}(t) = 2^{j/2}\varphi(2^j t - k)$ [17], where j is a scale parameter and k is a location parameter. Two different scaling functions, shown in Figure 1, are adopted in this work corresponding to values of $N = 3$ and 4, where N denotes the number of vanishing moments for that particular class of wavelets. The corresponding expansions for the response $x(t)$ and the excitation $f(t)$ are given by

$$x(t) = \sum_{k=I}^{J} \bar{\alpha}_k 2^{j/2}\varphi(2^j t - k) \tag{2}$$

and

$$f(t) = \sum_{k=I}^{J} \bar{\beta}_k 2^{j/2}\varphi(2^j t - k) \tag{3}$$

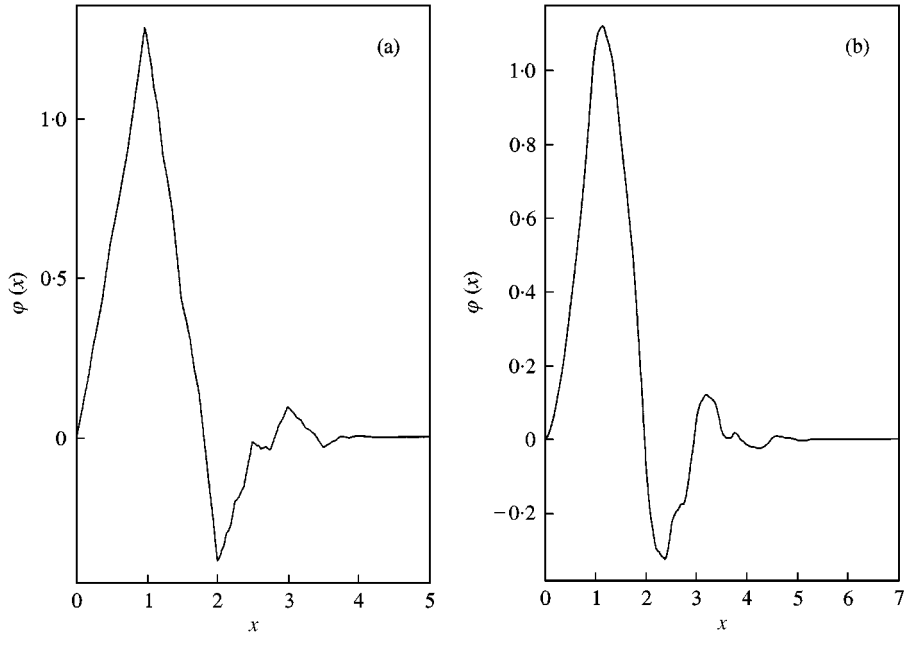

Figure 1. Daubechies scaling function with (a) $N = 3$ and (b) $N = 4$.

respectively. The lower and upper bounds I and J on the summations depend on the support of the specific Daubechies' scaling functions selected for the particular problem. If N is the number of vanishing moments, then the support of $\varphi_{j,k}(t) = 2^{j/2}\varphi(2^j t - k)$ is $[2^{-j}k, 2^{-j}(k + 2N - 1)]$, so that $I = k_0 - L + 2$ and $J = k_1 - 1$, where $L = 2N$, $k_0 = 2^j t_0$ and $k_1 = 2^j t_f$ are integer values and t_0 and t_f denote respectively, the initial and final time. The time derivatives of $x(t)$ can be expressed in terms of the corresponding time derivatives of the wavelet functions, resulting in the expressions

$$\dot{x}(t) = 2^j \sum_{k=I}^{J} \bar{\alpha}_k 2^{j/2} \dot{\varphi}(2^j t - k), \quad \ddot{x}(t) = 2^{2^j} \sum_{k=I}^{J} \bar{\alpha}_{j,k} 2^{j/2} \ddot{\varphi}(2^j t - k). \tag{4}$$

Substituting $\alpha_{j,k} = \bar{\alpha}_k 2^{j/2}$, $\beta_{j,k} = \bar{\beta}_k 2^{j/2}$ and $y = 2^j t$, and setting $t_0 = 0$, $t_f = 1$, the equation of motion can be rewritten as

$$m(y/2^j)2^{2j} \sum_{k=2-L}^{2^j-1} \alpha_{j,k} \ddot{\varphi}(y - k) + c(y/2^j)2^j \sum_{k=2-L}^{2^j-1} \alpha_{j,k} \dot{\varphi}(y - k)$$

$$+ k(y/2^j) \sum_{k=2-L}^{2^j-1} \alpha_{j,k} \varphi(y - k) = \sum_{k=2-L}^{2^j-1} \beta_{j,k} \varphi(y - k). \tag{5}$$

Taking the inner product of both sides of equation (5) with $\varphi(y - l)$, making the substitution $y - l = z$, and using the orthogonality of the translates of the scaling functions, results in the equation

$$m_l \sum_{k=2-L}^{2^j-1} \alpha_{j,k} \Gamma^{(2)}_{k-l} + c_l \sum_{k=2-L}^{2^j-1} \alpha_{j,k} \Gamma^{(1)}_{k-l} + k_l \alpha_{j,l} = \beta_{j,l}, \quad \text{for } l = 2 - L, \ldots, 2^j - 1, \tag{6}$$

where

$$\Gamma_k^{(n)} = \int_{-\infty}^{+\infty} \varphi^{(n)}(y-k)\varphi(y)\,\mathrm{d}y. \tag{7}$$

The terms $\Gamma_k^{(n)}$ in the latter expression denotes the so-called 2-term connection coefficients while φ^n is the nth derivative of the scaling function φ with respect to its argument. Analytical expressions for these coefficients, that can be computationally evaluated, have already been derived in the literature [18]. If the integral in equation (7) is evaluated over a finite domain, these coefficients can still be evaluated analytically [19] and they are referred to as the proper connection coefficients. The support of $\varphi(t)$ is the interval $[0, L-1]$ and it does not overlap with that of $\varphi^{(n)}(t-k)$ for $|k| \geqslant L-1$; therefore we have the following properties for the connection coefficients:

$$\Gamma_k^{(n)}(x) = 0 \quad \text{for } x \leqslant 0 \text{ or } x \leqslant k \text{ and } |k| \geqslant L-1\,, \tag{8}$$

$$\Gamma_k^{(n)}(x) = \Gamma_k^{(n)}(L-1) \quad \text{for } x \geqslant L-1. \tag{9}$$

Since $k, l = 2-L, \ldots, 2^{j-1}$, it follows that the only non-zero $\Gamma_k^{(n)}(x)$ with $x \neq L-1$ are those corresponding, in equation (6), to $l = 2-L, 3-L, \ldots, -1$ and for $l = 2^j - L + 2, 2^j - L + 3, \ldots, 2^j - 1$. In compact matrix notation equation (6) reduces simply to

$$\boldsymbol{\Gamma\alpha} = \boldsymbol{\beta}, \tag{10}$$

where $\boldsymbol{\Gamma}$ is a square matrix of dimension $2^j + L - 2$ in which are embedded all the properties of the system. If the solution to the initial-value problem is of interest, equation (10) can be solved for $\boldsymbol{\alpha}$ and the solution is then reconstructed as $x(y/2^j) = \sum_k \alpha_{j,k}\varphi(y-k)$ [20]. If the interest lies in solving the inverse problem, the set of algebraic equations in terms of the scaling function coefficients of the input and the output of equation (10) can be rearranged and solved for the unknown damping and stiffness parameters by means of the equation

$$\bar{\boldsymbol{\Gamma}}\boldsymbol{\theta} = \bar{\boldsymbol{\beta}}. \tag{11}$$

Assuming the mass to be known, the vector $\boldsymbol{\theta} = [c \;\; k]^{\mathrm{T}}$ contains the unknown parameters and a generic lth row of the $(2^j + L - 3) \times 2$ matrix $\bar{\boldsymbol{\Gamma}}$ reads

$$\bar{\Gamma}_l = \left[2^j \sum_k \alpha_{j,k} \Gamma_{k-1}^{(1)} \;\; \alpha_l \right]. \tag{12}$$

The corresponding lth term of the vector $\bar{\boldsymbol{\beta}}$ is given by

$$\bar{\beta}_l = \beta_l - 2^{2j} m_l \sum_k \alpha_{j,k} \Gamma_{k-l}^{(2)}. \tag{13}$$

Equation (11) has two unknowns, and as many equations as the number of scaling functions used in discretizing the governing differential equation. For a linear time-invariant system

TABLE 1

S.d.o.f. LTI system: influence of the level of resolution on the estimate accuracy; resolution level, $j = 9$

Resolution	$j = 7$		$j = 8$		$j = 9$	
$\hat{\theta}$	$\hat{c}$	$\hat{k}$	$\hat{c}$	$\hat{k}$	$\hat{c}$	$\hat{k}$
$\mu_{\hat{\theta}}$	1·26	39·02	1·26	39·00	1·26	39·00
$\text{COV}_{\hat{\theta}}$	1·35E-2	1·54E-3	2·71E-4	2·77E-5	4·7E-5	8·14E-6

(LTI) any two equations of the set (11) provide an estimate of the unknown parameters c and k. In general, however, for time-varying (LTV) systems, and due to the local nature of the scaling functions with support $s = L - 1$, the generic lth equation of the set (11) gives information about the system during the time interval t_{l-s-1}, t_{l+s-1}, where $t_i = i\Delta t$, Δt being the analysis time step. Thus, the evolution of the parameters over the whole duration of the analysis can be estimated by means of the above algorithm. This localization feature is peculiar to the choice of scaling functions to describe the signals, and is not shared by arbitrary basis functions. Indeed, the wavelet-based discretization is such that each equation from the set (11) corresponds to a time lag equal to $(s - 1)2\Delta t$. As previously mentioned, the support s is related to the resolution level by $[2^{-j}k, 2^{-j}(k + 2N - 1)]$, where k is the translation parameter and N characterizes the chosen Daubechies scaling function, and it diminishes in length as the resolution j increases. The lth entry in the vector $\boldsymbol{\theta}$ refers to the value taken by only one of the two unknown parameters over the corresponding lth time lag. Therefore, the only approximation introduced by solving for sequential pairs of equations is that the estimated parameters are assumed to be constant over time lags whose duration is given by $(s - 2)2\Delta t$ corresponding to two consecutive time steps. The system of equations given by equation (11) can also be solved by adopting a minimization technique, such as least squares, over groups of sequential equations. This is particularly important in the presence of noise or in the case where the underlying governing equation is known to be time varying or non-linear. In this case, the choice of the number of sequential equations over which to perform the least-squares minimization must be chosen with care, as it controls the sensitivity of the estimated parameters with respect to local features in the signal. These could be associated either with noise, or with abrupt changes in the parameters of the system. The analysis presented in this paper has been carried out adopting the Daubechies scaling functions with $N = 3$ and 4. The number of non-zero coefficients h_n involved in their construction are $L = 2N$. Table 1 shows the accuracy of the parameter estimate $\hat{\theta}$ for a LTI system. Values for the average, $\mu_{\hat{\theta}}$, over all times steps and the corresponding coefficient of variation ($\text{COV}_{\hat{\theta}} = \sigma_{\hat{\theta}}/\mu_{\hat{\theta}}$, for $\mu_{\hat{\theta}} \neq 0$, where σ represents the standard deviation) are shown in the table. The latter non-dimensional quantity is chosen as a measure of the dispersion of the estimates. The numerical values of the parameters of the system we are studying are $m = 1{\cdot}0$, $c = 1{\cdot}26$ and $k = 39{\cdot}0$. The excitation is given by $f(t) = A\sin(\omega_1 t) + A\sin(\omega_2 t)$, where $A = 10$, $\omega_1 = 6{\cdot}91$ rad/s and $\omega_2 = 5{\cdot}65$ rad/s.

2.2. MULTI-DEGREE-OF-FREEDOM SYSTEMS

The direct identification technique discussed in the previous section can be extended to multi-d.o.f. linear time-varying systems. Letting n be the number of d.o.f.s, the

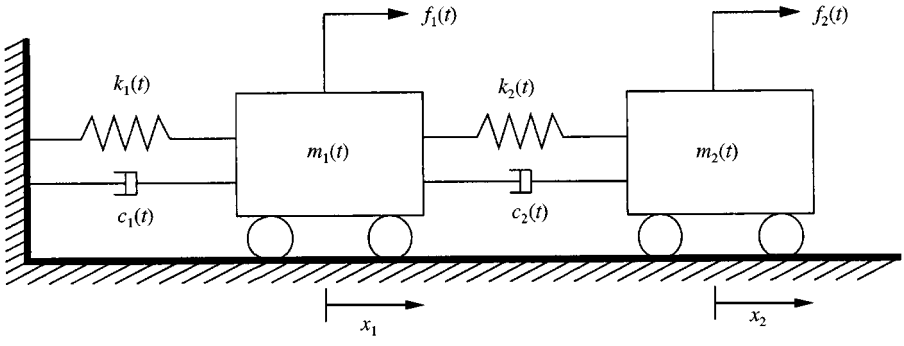

Figure 2. Schematic model of a 2-d.o.f. time-varying system.

Wavelet–Galerkin scheme is now applied to the resulting set of n coupled differential equations governing the problem, which are written as

$$\mathbf{M}(t)\ddot{\mathbf{x}} + \mathbf{C}(t)\dot{\mathbf{x}} + \mathbf{K}(t)\mathbf{x} = \mathbf{f}, \tag{14}$$

where the elements of the $n \times n$ matrices $\mathbf{M}(t)$, $\mathbf{C}(t)$ and $\mathbf{K}(t)$ represent time-varying physical masses, dashpots and springs. The $n \times 1$ matrices $\ddot{\mathbf{x}}$, $\dot{\mathbf{x}}$ and $\mathbf{x}$ are respectively time-varying acceleration, velocity and displacement responses, and the $n \times 1$ matrix $\mathbf{f}$ represents the generic time-varying external excitations.

In order to describe the extension of the procedure, a 2-d.o.f.s. system is considered and a sketch is shown in Figure 2. The various terms in equation (14) are given by

$$\mathbf{M} = \begin{bmatrix} m_1(t) & 0 \\ 0 & m_2(t) \end{bmatrix}, \quad \mathbf{C} = \begin{bmatrix} c_1(t) + c_2(t) & -c_2(t) \\ -c_2(t) & c_2(t) \end{bmatrix},$$

$$\mathbf{K} = \begin{bmatrix} k_1(t) + k_2(t) & -k_2(t) \\ -k_2(t) & k_2(t) \end{bmatrix}, \quad \mathbf{f} = \begin{bmatrix} f_1 \\ f_2 \end{bmatrix}. \tag{15}$$

The extension of equation (5) to the 2-d.o.f. case is obtained by expanding responses and forces time-histories in the wavelet bases adopting the same substitutions. Then, taking the inner product of both sides of the resulting equation with $\varphi(y - l)$, leads to the equations

$$m_{1,l}\sum_{I}^{J}\Gamma^{(2)}_{k-l}\alpha_{1,j,k} + (c_{1,l} + c_{2,l})\sum_{I}^{J}\Gamma^{(1)}_{k-l}\alpha_{1,j,k} + (k_{1,l} + k_{2,l})\alpha_{1,j,l}$$

$$- c_{2,l}\sum_{I}^{J}\Gamma^{(1)}_{k-l}\alpha_{2,j,k} - k_{2,l}\alpha_{2,j,l} = \beta_{1,j,l},$$

$$m_{2,l}\sum_{I}^{J}\Gamma^{(2)}_{k-l}\alpha_{2,j,k} + c_{2,l}\sum_{I}^{J}\Gamma^{(1)}_{k-l}\alpha_{2,j,k} + k_{2,l}\alpha_{2,j,l}$$

$$- c_{2,l}\sum_{I}^{J}\Gamma^{(1)}_{k-l}\alpha_{1,j,k} - k_{2,l}\alpha_{1,j,l} = \beta_{2,j,l} \tag{16}$$

The latter equations can be expressed in matrix notation in a similar form to equation (11) by introducing a system matrix $\bar{\mathbf{\Gamma}}$ which, in general, has dimension $n2^j \times pn$, when n is the number of d.o.f. and p is the number of unknown parameters per d.o.f. Assuming both masses to be known, the generic lth couple of rows to be solved for the estimate of damping and stiffness parameters is given by

$$\begin{bmatrix} \sum_I^J \Gamma^{(1)}_{k-l}\alpha_{1,j,k} & \alpha_{1,j,l} & \sum_I^J \Gamma^{(1)}_{k-l}(\alpha_{1,j,k}-\alpha_{2,j,k}) & \alpha_{1,j,l}-\alpha_{2,j,l} \\ 0 & 0 & \sum_I^J \Gamma^{(1)}_{k-l}(\alpha_{2,j,k}-\alpha_{1,j,k}) & \alpha_{2,j,l}-\alpha_{1,j,l} \end{bmatrix} \begin{bmatrix} c_{1,l} \\ k_{1,t} \\ c_{2,l} \\ k_{2,l} \end{bmatrix}$$

$$= \begin{bmatrix} \beta_{1,j,l} & -m_1 \sum_I^J \Gamma^{(2)}_{k-l}\alpha_{1,j,k} \\ \beta_{2,j,l} & -m_2 \sum_I^J \Gamma^{(2)}_{k-l}\alpha_{2,j,k} \end{bmatrix}. \tag{17}$$

The resulting set of algebraic equations can be solved either by considering sequential groups of $2n$ equations or by minimizing an associated measure of the error. The approximation introduced in the estimation procedure is the same as that discussed for the s.d.o.f. case. It must be emphasized that the direct identification scheme described above does not require the uncoupling of the governing set of equations in order to estimate the unknown parameters. It is emphasized that the procedure is consistent with the assumption that the parameters are constant over a time interval strictly linked to the support of the scaling functions and which diminishes in length as the resolution j increases. It will be shown that the above-mentioned assumption is not restrictive; indeed in the following sections the identification procedure will be applied to systems featuring different idealized evolutions of their mechanical parameters. The latter consideration constitutes the main difference with respect to STFT methods where the changes in the frequency content of a signal have to be slow relative to the smallest frequency resolved by the Fourier transform, i.e., $2\pi/T$, where T is the length of the time window. Moreover, it is well known that in order to assure a meaningful Fourier analysis such length cannot be taken too small therefore enforcing restrictive assumptions on the nature of the parameter variations. The effect of the level of resolution on the accuracy of the parameter estimates has been evaluated for a 2.d.o.f. LTI system; the results are shown in Table 2. The system is excited at both co-ordinates by the same sinusoidal force used for the s.d.o.f. case; the numerical values of the parameters are $m_1 = 1{\cdot}0$ and $m_2 = 2{\cdot}0$, $c_1 = 1{\cdot}26$ and $c_2 = 1{\cdot}1$, $k_1 = 39{\cdot}0$ and $k_2 = 35{\cdot}0$.

3. ROBUSTNESS OF THE PROCEDURE WITH RESPECT TO NOISY DATA

This section deals with the identification of the parameters of dynamical system terms based on noise-corrupted input/output data. In order to tackle the problem, the wavelet transform (WT) is employed at two stages. Initially, the data are pre-processed by means of the WT, then the same transform is applied to the functionals involved in the identification algorithm. The spatial localization of the wavelets turns out to be also convenient in processing the data in order to filter out the noise. In fact, the wavelet bases allow the

TABLE 2

2-d.o.f LTI system: influence of the level of resolution on the estimate accuracy; resolution level, $j = 9$

Resolution	$j = 7$		$j = 8$		$j = 9$	
	$\mu_{\hat{\theta}}$	$\mathrm{COV}_{\hat{\theta}}$	$\mu_{\hat{\theta}}$	$\mathrm{COV}_{\hat{\theta}}$	$\mu_{\hat{\theta}}$	$\mathrm{COV}_{\hat{\theta}}$
$\hat{c}_1$	1·257	0·548	1·26	0·012	1·26	4·4E-4
$\hat{k}_1$	38·99	0·051	39·0	2·0E-3	39·0	9·3E-5
$\hat{c}_2$	1·10	0·40	1·10	5·25E-3	1·10	9·0E-5
$\hat{k}_2$	35·03	0·26	35·0	3·6E-3	35·0	5·59E-5

detection of the occurrence time of a significant change in the analyzed function by looking at the values of its wavelet coefficients at level $j = j_0, \ldots, J$ at spatial indices k with $k2^{-j} \approx t$. It is important to determine whether such a change is associated with an actual physical event or it is merely induced by noise. The denoising task can then be interpreted as that of extracting and modifying in a suitable way those coefficients associated with changes in the signal that are also consistent with the specific definition of noise given by the thresholding algorithm. Different methods for identifying and either modifying or removing these coefficients have been developed recently in the signal processing community [21–23]. The approach that is considered in this section consists of building an adaptive algorithm based on the principle of selective wavelet reconstruction [21]. Thus, expressing the wavelet transform of the data $y = (y_i)_{i=1}^{2^j}$ as

$$y = \sum_{j,k} w_{j,k} W_{jk}, \tag{18}$$

where $w_{j,k}$ are the wavelet coefficients, a finite list δ of (j, k) pairs is introduced, along with a projection operator, $T(.,\delta)$, defined as

$$T(y, \delta) = \sum_{(j,k)\in\delta} w_{j,k} W_{jk}. \tag{19}$$

The operator $T(.,\delta)$ provides an approximation of the data y by selecting only a subset of the wavelet coefficients. Given the contaminated data,

$$y_i = x(t_i) + \varepsilon_i, \quad i = 1, \ldots, 2^j, \tag{20}$$

where ε_i are independently distributed zero-mean Gaussian random variables with standard deviation σ, and $x(\cdot)$ is the target function. It follows that the orthogonal transform $z = W\varepsilon$ of ε_i is also a white noise and the wavelet coefficients are given by

$$w_{j,k} = \theta_{j,k} + z_{j,k}, \tag{21}$$

where $\theta = Wx$. From the previous consideration it follows that while every wavelet coefficient contributes noise, only few of them contribute to the signal. In order to select the

latter coefficients, a number of thresholding rules have been proposed according to different criteria. In our simulations, the best performance has been obtained with the following simple thresholding [21],

$$\eta(w, \lambda) = wI\{|w| > \lambda\}, \tag{22}$$

where $I\{\cdot\}$ denotes a set function, equal to 1 if its argument is true, and 0 if it is false, and λ is some threshold level. This thresholding logic leads to an estimator $\hat{\theta}_{j,k}$ of the wavelet coefficients $\theta_{j,k}$ in equation (21) given by

$$\hat{\theta}_{j,k} = w_{j,k} I\{|w_{j,k}| > \lambda_n \sigma\}, \tag{23}$$

where $\lambda_n = (2 \log n)^{1/2}$. The noise level σ is taken as the standard deviation of the coefficients at the finest scale J based on the assumption that these coefficients are mainly associated with pure noise, and n denotes the number of coefficients at that scale. The selective wavelet reconstruction $T(y, \delta)$ of equation (19) can now be expressed as

$$T = W^{\mathrm{T}} \circ E \circ W, \tag{24}$$

where E denotes the diagonal linear projection of equation (22). Therefore, equation (24) gives the approximation $\hat{y}$ of the data y by applying the wavelet transform, followed by diagonal linear projection, followed by the inverse wavelet transform. The above criterion has also been compared to a simpler one where the estimator of equation (23) has been replaced by

$$\hat{\theta}_{j,k} = \begin{cases} w_{j,k} & \text{if } j < \bar{j}, \\ 0 & \text{if } j \geqslant \bar{j}, \end{cases} \tag{25}$$

meaning that all the wavelet coefficients beyond a selected scale $\bar{j}$, which is related to the analyzed function, are set to zero.

Figure 3 shows the resulting filtered signal obtained by applying both of the above wavelet reconstruction strategies to noisy data. Referring to the general case of an n-dimensional measurement vector $\mathbf{y}$, such noisy data are obtained by adding a Gaussian white noise $\boldsymbol{\varepsilon}$ assumed proportional to the measurement vector

$$\boldsymbol{\varepsilon} = \mathbf{S}\mathbf{y}, \tag{26}$$

where $\mathbf{S}$ is an $n \times n$ diagonal random matrix whose diagonal components $s_1, \ldots, s_n$ are independent and identically distributed with zero means and standard deviations σ. The latter quantity represents the noise-to-signal ratio of the measurements at each time instant $i\Delta t_I$, where Δt_I is the identification interval. In order to measure the effect of the selective wavelet reconstruction described above on the accuracy of the parameters estimates, the following quantities are introduced:

$$\mathrm{err}_i(k) = \frac{k_{i,true} - \hat{k}_i}{k_{i,true}} \times 100 \quad \mathrm{err}_i(c) = \frac{c_{i,true} - \hat{c}_i}{c_{i,true}} \times 100, \tag{27}$$

measuring the error at the ith time step between estimated and actual model parameters. The introduction of the thresholding of the wavelet coefficients of the signals has to be taken

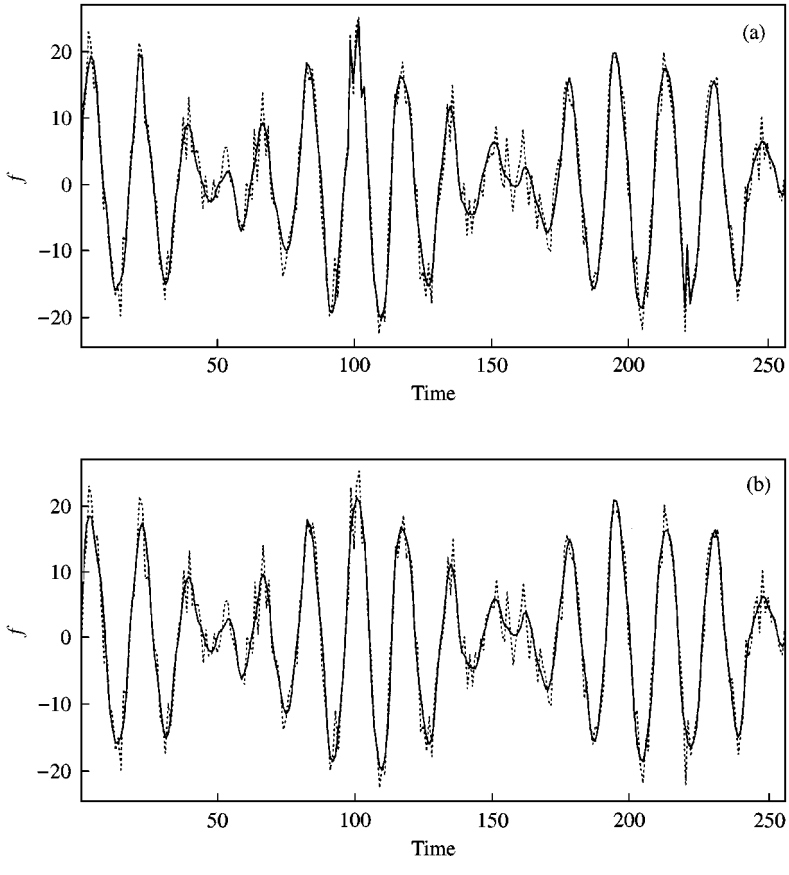

Figure 3. Denoised signal according to different denoising strategies with $\sigma = 10\%$: (a) corresponds to equation (23); (b) corresponds to equation (25).

into account when performing the least-squares estimate of the unknown parameters. Indeed, by removing the wavelet coefficients associated with the higher scales, a correlation in the initially uncorrelated ε_i is introduced. Thus, the initial diagonal covariance matrix $\sigma\mathbf{I}$ of ε_i, where $\mathbf{I}$ is the identity matrix of order 2^j, becomes a new matrix $\mathbf{Q}$ of the same order with, in general, non-zero off-diagonal terms. Such a matrix has to be evaluated and considered through the so-called weighted least-squares scheme. Considering the continuous form of the scaling function expansion of the measured response $y(t)$, the kth scaling function coefficient is given by

$$\bar{\alpha}_k = \int_0^T y(t)\varphi_k(t)\,\mathrm{d}t = \int_0^T x(t)\varphi_k(t)\,\mathrm{d}t + \int_0^T \varepsilon(t)\varphi_k(t)\,\mathrm{d}t, \tag{28}$$

with $\varphi_k(t) = 2^{j/2}\varphi(2^j t - k)$, where the scale index j is omitted. Letting $l\Delta t$ represent the time lag equal to the scaling function support $l = L - 1$, equation (28) may be rewritten as $\tilde{\alpha}_k = \alpha_k + \zeta_k$ with

$$\alpha_k = \int_{t_k}^{t_k + l\Delta t} x(t)\varphi_k(t)\,\mathrm{d}t, \quad \zeta_k = \int_{t_k}^{t_k + l\Delta t} \varepsilon(t)\varphi_k(t)\,\mathrm{d}t, \tag{29}$$

where the term ζ_k is a random scaling function coefficient. Multiplying the latter coefficient by ζ_{k+1} and taking expectations $E[\cdot]$, results in

$$E[\zeta_k \zeta_{k+1}] = \int\int_{t_k}^{t_{k+1}+l\Delta t} E[\varepsilon(t)\varepsilon(\tau)]\,\varphi_k(t)\,\varphi_{k+1}(\tau)\,\mathrm{d}t\,\mathrm{d}\tau. \tag{30}$$

If the measurement noise is assumed to consist of a sequence of uncorrelated random variables, then the orthogonality of the scaling functions results in $E[\zeta_k \zeta_i] = \sigma^2 \delta_{k,i}$, which yields a diagonal covariance matrix and implies that the least-squares estimates $\hat{\boldsymbol{\theta}}$, obtained by minimizing with respect to $\boldsymbol{\theta}$ the quantity $\| \bar{\boldsymbol{\beta}} - \bar{\boldsymbol{\Gamma}} \boldsymbol{\theta} \|^2$, are unbiased estimates of $\boldsymbol{\theta}$. Alternatively, if a selective wavelet reconstruction is performed, as indicated by equation (23) and (25), the original purely random process representing the measurement noise becomes a band-limited white noise whose autocovariance function assumes the form

$$E[\varepsilon(t_k)\varepsilon(t_i)] = \sigma^2 \frac{\sin[2\pi B(t_k - t_i)]}{2\pi B(t_k - t_i)}. \tag{31}$$

The latter expression modifies equation (30) which becomes

$$E[\zeta_k \zeta_{k+1}] = \sigma^2 \int\int_{t_k}^{t_k + (l-1)\Delta t} \frac{\sin[2\pi B(t_k - t_i)]}{2\pi B(t_k - t_i)}\,\varphi_k(t)\,\varphi_{k+1}(\tau)\,\mathrm{d}t\,\mathrm{d}\tau, \tag{32}$$

where B represents the bandwidth and is given by $B = 1/(2\Delta t_I 2^{J-\tilde{J}})$. Based on equation (32), the sparse noise covariance matrix $\mathbf{Q}$ is obtained as $\mathbf{Q} = E(\boldsymbol{\zeta}\boldsymbol{\zeta}^{\mathrm{T}})$, where $\boldsymbol{\zeta} = \{\zeta_1, \ldots, \zeta_{2j}\}^{\mathrm{T}}$. Consequently, $\mathbf{Q}$ being invertible, the resulting weighted least-squares scheme consists of minimizing the quadratic form

$$V(\boldsymbol{\theta}) = (\bar{\boldsymbol{\beta}} - \bar{\boldsymbol{\Gamma}}\boldsymbol{\theta})^{\mathrm{T}} \mathbf{Q}^{-1} (\bar{\boldsymbol{\beta}} - \bar{\boldsymbol{\Gamma}}\boldsymbol{\theta}), \tag{33}$$

leading to the generalized normal equations

$$(\bar{\boldsymbol{\Gamma}}^{\mathrm{T}} \bar{\boldsymbol{\Gamma}})\,\hat{\boldsymbol{\theta}} = \bar{\boldsymbol{\Gamma}}^{\mathrm{T}} \mathbf{Q}^{-1} \bar{\boldsymbol{\beta}}. \tag{34}$$

In order to extend the noise statistical characterization, further analyses, aimed at clarifying the role of the noise on the proposed identification algorithm, have been conducted. Towards this goal, the effect of the wavelet-based linear transformation on the perturbed signals will be briefly discussed. In view of its simplicity, the s.d.o.f case will be used to extend the analysis from the previous section to treat noisy data. The generic lth row of the matrix $\bar{\boldsymbol{\Gamma}}$ in the algebraic problem given by equation (11) becomes

$$\bar{\Gamma}_l = \left[2^j \left(\sum_k \Gamma^{(1)}_{k-l} \alpha_k + \sum_k \Gamma^{(1)}_{k-l} \zeta_k \right) \quad \alpha_1 + \zeta_l \right], \tag{35}$$

where the coefficients ζ_l and α_l are as defined in equation (29). The lth term on the right-hand side of equation (11) becomes

$$\tilde{\beta}_l = \bar{\beta}_l - 2^{2j} m \sum_k \Gamma^{(2)}_{k-l} \zeta_{j,k} \tag{36}$$

Where $\bar{\beta}_1$ is given by equation 13.

Thus, in order to account for noisy data, equation (11) is modified according to

$$\boldsymbol{\Gamma}\boldsymbol{\theta} + \tilde{\boldsymbol{\Gamma}}\boldsymbol{\theta} = \tilde{\boldsymbol{\beta}}, \tag{37}$$

where the two operators $\boldsymbol{\Gamma}$ and $\tilde{\boldsymbol{\Gamma}}$ refer respectively, to the unperturbed quantity and its random perturbation. The mean vector and covariance matrix of $\tilde{\boldsymbol{\beta}}$ are given respectively by

$$E[\tilde{\boldsymbol{\beta}}] = E[\boldsymbol{\Gamma}\boldsymbol{\theta} + \tilde{\boldsymbol{\Gamma}}\boldsymbol{\theta}] = E[\boldsymbol{\Gamma}\boldsymbol{\theta}] + E[\tilde{\boldsymbol{\Gamma}}\boldsymbol{\theta}] = \boldsymbol{\Gamma}\boldsymbol{\theta} \tag{38}$$

and

$$E[(\tilde{\boldsymbol{\beta}} - E[\tilde{\boldsymbol{\beta}}])(\tilde{\boldsymbol{\beta}} - E[\tilde{\boldsymbol{\beta}}])^{\mathrm{T}}] = E[(\tilde{\boldsymbol{\Gamma}}\boldsymbol{\theta})(\tilde{\boldsymbol{\Gamma}}\boldsymbol{\theta})^{\mathrm{T}}] = E[\tilde{\boldsymbol{\Gamma}}\boldsymbol{\theta}\boldsymbol{\theta}^{\mathrm{T}}\tilde{\boldsymbol{\Gamma}}^{\mathrm{T}}]. \tag{39}$$

The covariance of $\tilde{\boldsymbol{\beta}}$ depends therefore in a non-linear fashion on the parameters, a fact that considerably complicates the computational task of optimization. Equation (39) can be rewritten using the trace operator as

$$E[\tilde{\boldsymbol{\Gamma}}\boldsymbol{\theta}\boldsymbol{\theta}^{\mathrm{T}}\tilde{\boldsymbol{\Gamma}}^{\mathrm{T}}] = \mathrm{Tr}(\boldsymbol{\theta}\boldsymbol{\theta}^{\mathrm{T}})\, E[\tilde{\boldsymbol{\Gamma}}^{\mathrm{T}}\tilde{\boldsymbol{\Gamma}}]. \tag{40}$$

Therefore, equation (37) can be rewritten in the more convenient form

$$\mathbf{b} = \boldsymbol{\Gamma}\boldsymbol{\theta} + \varepsilon, \tag{41}$$

where ε represents a random vector with $E[\varepsilon] = \mathbf{0}$ and covariance $\mathbf{R}_\varepsilon = \mathbf{R}(\boldsymbol{\theta})$ given by equation (40), so that $\mathbf{b} = \mathrm{N}(\boldsymbol{\Gamma}\boldsymbol{\theta}, \mathbf{R}(\boldsymbol{\theta}))$ and the joint probability density function of the random vector $\mathbf{b}$, whose dimension is $N = 2^j$, is given by

$$P(\mathbf{b}) = \frac{1}{(2\pi)^{N/2}(\det \mathbf{R}(\boldsymbol{\theta}))^{1/2}} \exp\left\{-\frac{1}{2}[(\mathbf{b} - \boldsymbol{\Gamma}\boldsymbol{\theta})^{\mathrm{T}}\mathbf{R}(\boldsymbol{\theta})^{-1}(\mathbf{b} - \boldsymbol{\Gamma}\boldsymbol{\theta})]\right\}. \tag{42}$$

Although the considerations developed so far lead to conclude that the estimate of the parameters vector $\boldsymbol{\theta}$ could still be carried out through a least-squares scheme, the non-linear dependence of the covariance matrix $\mathbf{R}(\boldsymbol{\theta})$ on the parameter vector $\boldsymbol{\theta}$ in equation (42) involves considerable difficulties. In order to overcome such difficulties, a different approach can be followed that involves analyzing the effect of the operator $\tilde{\boldsymbol{\Gamma}}$ on the identification algorithm. The scaling coefficients α_k in equation (35) are those obtained from the selective wavelet reconstruction; however, the effect of the operator $\tilde{\boldsymbol{\Gamma}}$, arising from the presence of noise, is to amplify the wavelet coefficients of the whole term $\boldsymbol{\Gamma} + \tilde{\boldsymbol{\Gamma}}$ at the finest scales. In other words, even if the denoised signal contains apparently negligible noise contributions, the identification of the parameters can still be poor because the high-frequency content of $\boldsymbol{\Gamma}$ is significantly amplified by the perturbation introduced by $\tilde{\boldsymbol{\Gamma}}$ which features the time derivatives of the noise component.

Figure 4 shows the effect of noise on the finest scale wavelet coefficients of the terms

$$\gamma^{(1)} = \sum_k \Gamma^{(1)}_{k-l}(\alpha_k + \zeta_k) \tag{43}$$

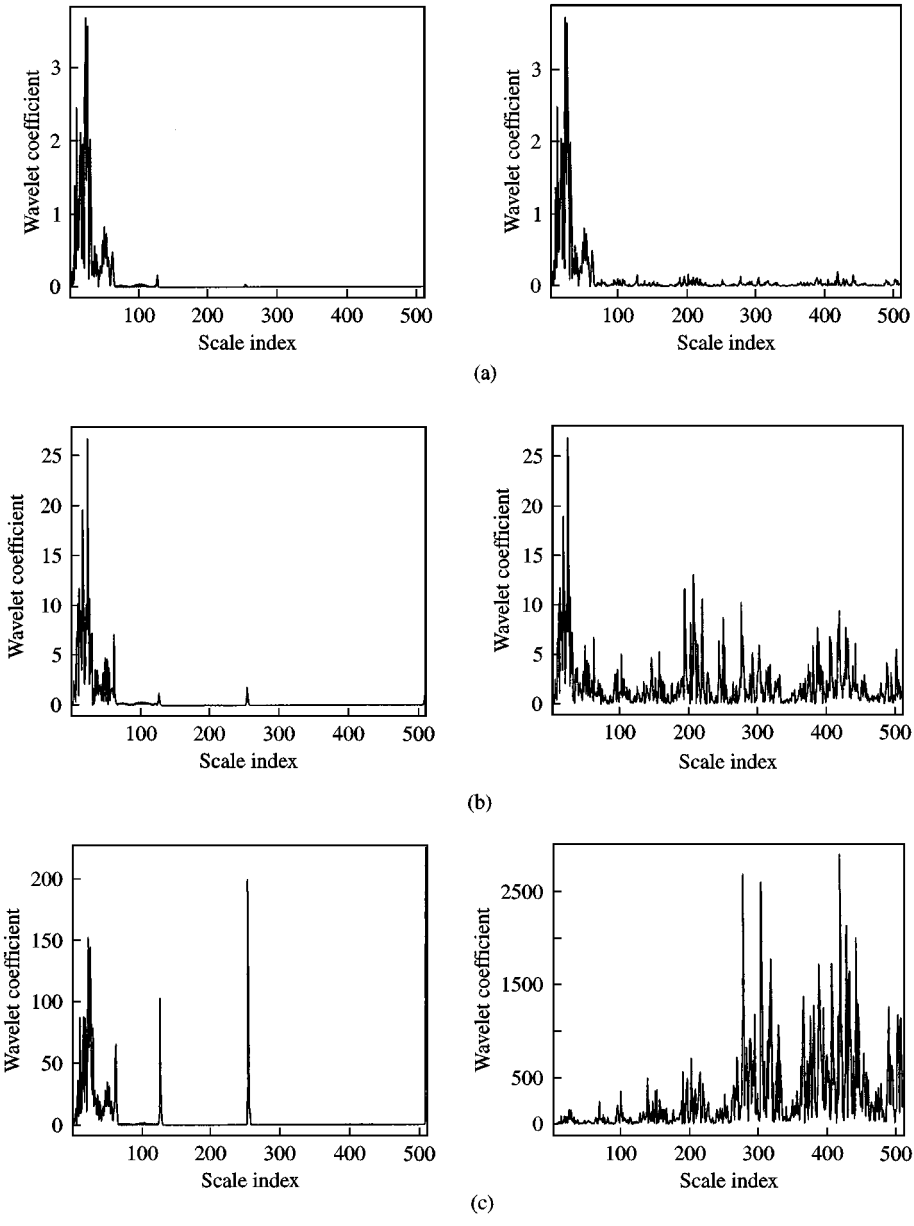

Figure 4. Amplification of higher scales wavelet coefficients through time-differentiation of the signal: (a) wavelet coefficients of signal; (b) wavelet coefficients of first derivative (equation (43)); (c) wavelet coefficients of second derivative (equation (44)). Left column: noiseless data; right column: noisy data, $\sigma = 10\%$.

and

$$\gamma^{(2)} = \sum_k \Gamma^{(2)}_{k-l}(\alpha_k + \zeta_k), \tag{44}$$

appearing in expressions (35, 36). The resolution is $J = 9$ and the abscissa index refers to the wavelet coefficients position across the scales; thus, going from right to left, the last

$2^{J-1} = 256$ points correspond to the coefficients at scale 8, the following $2^{j-2} = 128$ points correspond to the coefficients at scale 7 and so on. In order to mitigate the effect of amplifying the noise through differentiation, the thresholding strategy has been extended to the terms $\gamma^{(1)}$ and $\gamma^{(2)}$. Thus, in addition to thresholding the input/output data, the terms $\gamma^{(1)}$ and $\gamma^{(2)}$ are also subjected to a similar thresholding.

4. NUMERICAL INVESTIGATIONS

The numerical investigations that are shown in this section refer to stable systems characterized by time-dependent behavior of their mechanical parameters. Three ideal cases of time variation are studied, namely slow, abrupt and periodic variations. The identification is carried out for each of the systems under both free and forced oscillations taking into account noise-corrupted data. The response of the systems used to perform the identification is obtained from numerical solutions of the governing differential equations using a fifth order Runge–Kutta–Verner method. For the ideal cases without noise, the estimates of the parameters were obtained by solving, sequentially, pairs of equations. In presence of noise the estimates were obtained by a least-squares solution of subsets of the governing equations, thus yielding estimates of the average behavior of the parameters over a time window covered by that particular subset. The number of equations entering such subsets will be specified for each case analyzed.

4.1. SMOOTHLY VARYING PARAMETERS

The first analysis is addressed to the identification of the mechanical properties of an ideal model that could be interpreted as a representation of a degrading structure. The simulation is based on quadratic variations in time of both stiffness and damping. The former is assumed to be decaying while the latter is increasing. As already pointed out, the value of the parameter in time is estimated either by taking sequential pairs of equations or by taking the least-squares solution over sequential subsets of equations. The sampling rate of the analysis is $\Delta t = 0{\cdot}04$ s and the level of resolution is $j = 9$. The stiffness and damping variations for the s.d.o.f. case are given by

$$c(t) = c_0 + at^2, \quad k(t) = k_0 + bt^2,$$

where $c_0 = 1{\cdot}26$, $k_0 = 39{\cdot}0$, $a = 0{\cdot}001$ and $b = -0{\cdot}01$. The excitation is given by $f(t) = A\sin(\omega_1 t) + A\sin(\omega_2 t)$, where $A = 1{\cdot}0$, $\omega_1 = 6{\cdot}91$ rad/s and $\omega_2 = 5{\cdot}65$ rad/s. The initial conditions for the free vibration case are $x_0 = 0{\cdot}1$ and $\dot{x}_0 = 0{\cdot}0$

The results for the s.d.o.f are shown in Table 3. A 2-d.o.f system is also considered, with the same excitation acting on each of its d.o.f as that in the previous case; the initial conditions for the free vibrations analysis are $x_{1,0} = 0{\cdot}0$, $\dot{x}_{1,0} = 0{\cdot}0$, $x_{2,0} = 0{\cdot}1$, $\dot{x}_{2,0} = 0{\cdot}0$. The quadratic laws governing the time variations of the parameters are the same as the previous case with the initial values of the parameters given as $c_{1,0} = 1{\cdot}26$, $k_{1,0} = 39{\cdot}0$, $c_{2,0} = 1{\cdot}1$, $k_{2,0} = 35{\cdot}0$. The results for the 2-d.o.f. are shown in Table 4.

The results with noisy data refer to estimates obtained through least-squares solutions over sequential subsets of 64 equations. The least-squares solutions have proven to improve the tracking of the parameters in the presence of noisy data. Figures 5 and 6 show the tracking of the parameters for respectively, the s.d.o.f and 2-d.o.f. systems both excited by the previously defined harmonic force. The results show that the procedure allows for rather

TABLE 3

LTV s.d.o.f.: monotonically varying parameters; estimate accuracy expressed as r.m.s. (err(·)) for increasing level of noise σ; resolution level, j = 9

	Forced oscillations		Free oscillations	
σ	*err*(*c*)	*err*(*k*)	*err*(c)	*err*(*k*)
0	0·324	0·053	0·374	0·045
5%	8·72	2·44	6·39	2·18
10%	12·77	3·95	11·75	3·52

TABLE 4

LTV 2-d.o.f.: monotonically varying parameters; estimate accuracy expressed as r.m.s. (err(·)) for increasing level of noise σ; resolution level, j = 9

	Forced oscillations				Free oscillations			
σ	$err(c_1)$	$err(k_1)$	$err(c_2)$	$err(k_2)$	$err(c_1)$	$err(k_1)$	$err(c_2)$	$err(k_2)$
0	0·33	0·047	0·33	0·05	0·76	0·068	0·85	0·077
5%	8·72	2·59	5·57	1·51	7·26	1·33	8·91	2·37
10%	18·66	4·5	14·72	2·74	23·53	3·23	30·45	4·95

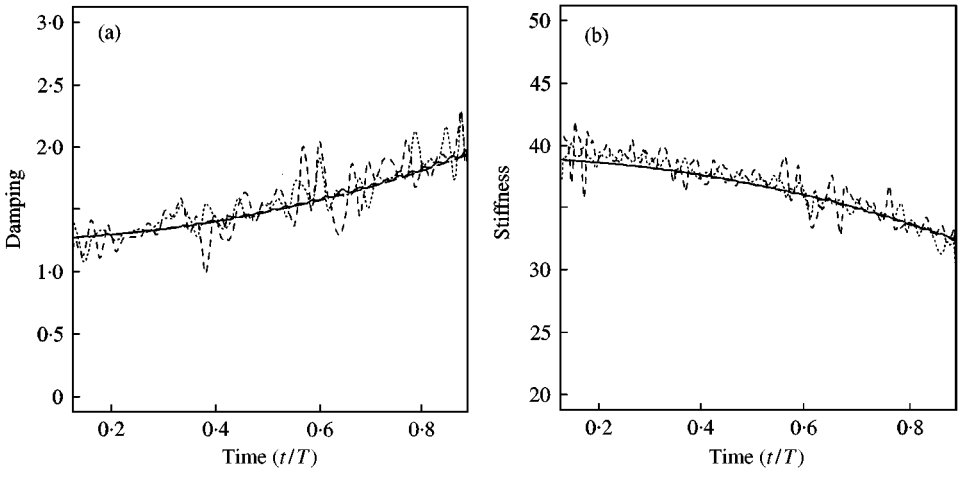

Figure 5. LTV s.d.o.f. system: slowly varying (a) damping and (b) stiffness estimates; —, true; ····, 5%; - - -, 10%; – – –, no noise.

robust stiffness estimates whose error root mean square (r.m.s) value is always lower than 5% for both the s.d.o.f and 2-d.o.f cases. The damping estimates are less robust to noise levels, showing an error r.m.s. value ranging from 10% for the s.d.o.f case to a maximum value of 30% for the 2-d.o.f. case. Forced and free vibration cases provide similar estimation

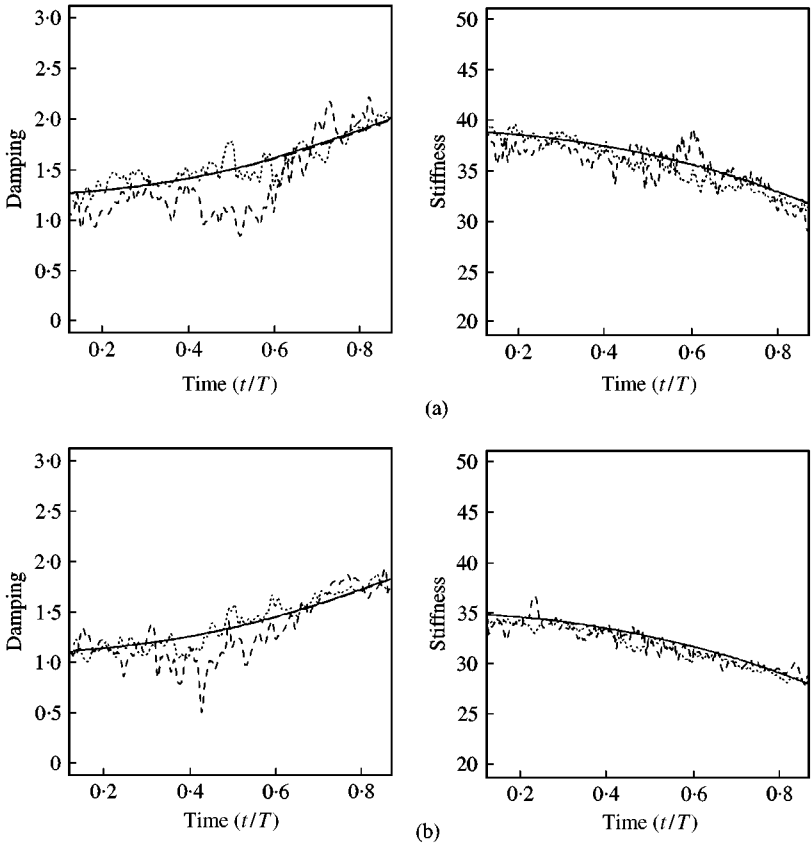

Figure 6. LTV 2-d.o.f. system: slowly varying damping (left column) and stiffness (right column) estimates: (a) first element (b) second element. ——, true; ····, 5%; - - -, 10%; – – –, no noise.

accuracy with the exception of the damping estimates which are more accurate under forced vibration.

4.2. PERIODICALLY VARYING PARAMETERS

The second set of numerical investigations concerns a system characterized by a parametrically varying stiffness. The time step is $\Delta t = 0{\cdot}046$ s and the resolution level is $j = 9$. The s.d.o.f. case considered is governed by the damped Mathieu equation,

$$m\ddot{x}(t) + c\dot{x}(t) + (k_0 - q\cos\Omega t)x(t) = f(t),$$

where $c = 1{\cdot}26$, $k_0 = 39{\cdot}0$; $q = 5{\cdot}0$ is the parameter measuring the strength of the parameteric excitation whose frequency is $\Omega = 0{\cdot}4$ and $f(t)$ is the same as the previous example. The initial conditions for the free vibrations are $x(0) = 0{\cdot}1$, $\dot{x}(0) = 0{\cdot}0$. Setting $k(t) = k_0 - q\cos\Omega t$, the estimate of the evolution of the periodic parameter $k(t)$ is given in Figure 7. The estimate accuracy is evaluated through the r.m.s. value of the errors defined in equation (40) and the numerical values are given in Table 5.

For the 2-d.o.f. system considered next, the excitation acting on each d.o.f. is the same as the previous s.d.o.f. case; the initial conditions for the free vibrations analysis are $x_{1,0} = 0{\cdot}0$,

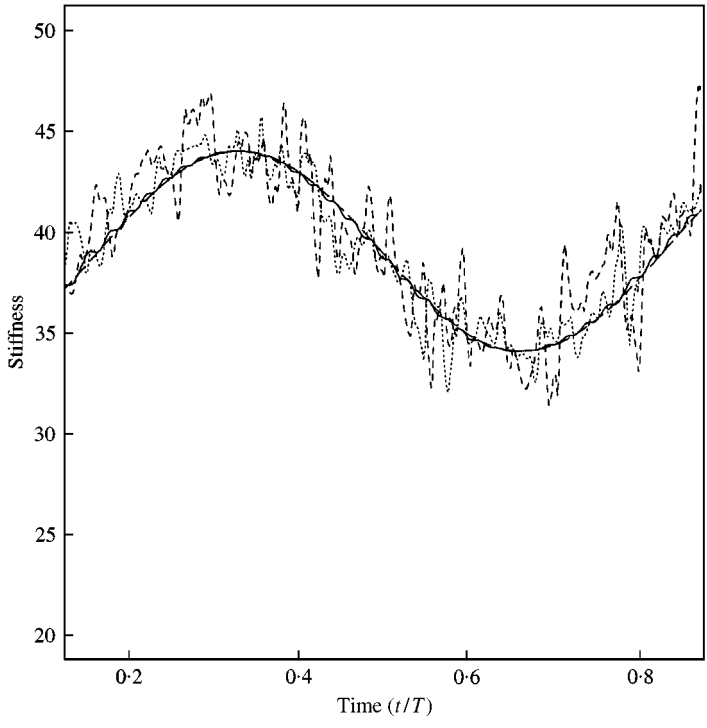

Figure 7. LTV s.d.o.f. system: periodically varying stiffness estimates. ——, true; ····, 5%; - - -, 10%; – – –, no noise.

TABLE 5

LTV s.d.o.f.: Periodically varying parameters; estimate accuracy expressed as r.m.s. (err(·)) for increasing level of noise σ; resolution level, j = 9

	Forced oscillations		Free oscillations	
σ	*err*(*c*)	*err*(*k*)	*err*(*c*)	*err*(*k*)
0	2·17	0·38	1·68	0·33
5%	15·02	3·07	17·64	3·35
10%	16·04	5·22	20·72	4·88

$\dot{x}_{1,0} = 0{\cdot}0$, $x_{2,0} = 0{\cdot}1$, $\dot{x}_{2,0} = 0{\cdot}0$. The time-periodic parameters are specified as $k_1(t) = k_{1,0} - q \sin \Omega t$, $k_2(t) = k_{2,0} - q \cos \Omega t$ with $k_{1,0} = 39{\cdot}0$, $k_{2,0} = 35{\cdot}0$, $q = 5{\cdot}0$ and $\Omega = 0{\cdot}4$. The damping coefficients are constant for both d.o.f.s. and their values are $c_1 = 1{\cdot}26$, $c_2 = 1{\cdot}1$. The results are given in Table 6.

In the presence of noise, the estimates for both systems have been obtained through least-squares solutions over sequential subsets of 48 equations. The results obtained for the periodic parameter variation cases are consistent with the quadratic variation cases shown in the previous example. The estimates evolution for increasing level of noise is presented in Figure 8.

TABLE 6

LTV 2-d.o.f.: periodically varying parameters; estimate accuracy expressed as r.m.s. (err(·)) for increasing level of noise σ; resolution level, j = 9

	Forced oscillations				Free oscillations			
σ	$err(c_1)$	$err(k_1)$	$err(c_2)$	$err(k_2)$	$err(c_1)$	$err(k_1)$	$err(c_2)$	$err(k_2)$
0	2·0	0·24	2·21	0·27	4·55	0·33	5·8	0·41
5%	12·57	2·82	10·75	2·83	17·22	2·5	22·5	3·52
10%	20·13	4·77	18·29	3·14	37·96	3·91	48·23	5·74

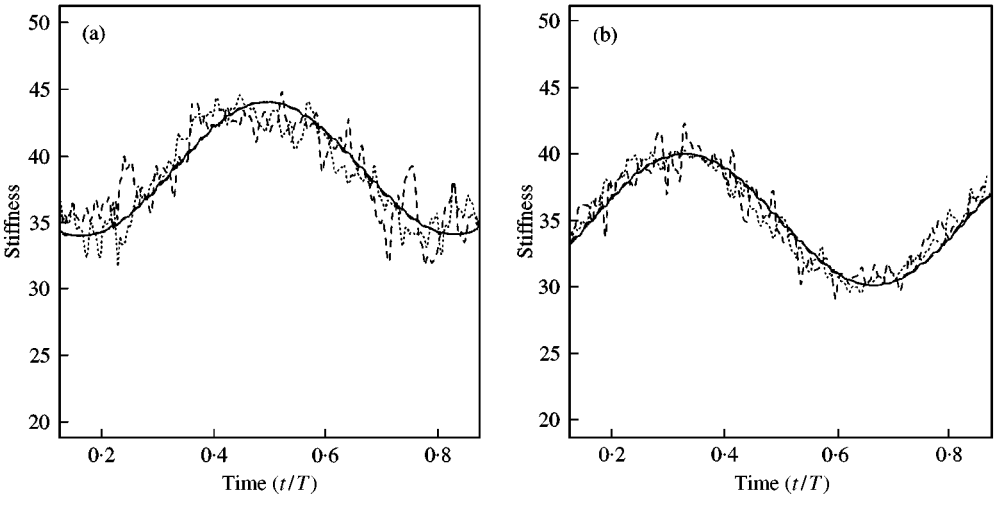

Figure 8. LTV 2-d.o.f. system: periodically varying stiffness estimates; (a) first element; (b) second element. ——, true; ····, 5%; – – –, 10%; – – –, no noise.

4.3. ABRUPT STIFFNESS VARIATIONS

The case considered in this subsection consists of an idealized model of damage characterized by an abrupt change in the stiffness. Its purpose is to assess the suitability of the identification procedure to abrupt variations in the parameters. The choice of the number of equations included in the least-squares solution is crucial in order to detect both the amplitude and the time of ocurrence of the variation of stiffness. The larger the number of equations used in the least-squares procedure, the smaller the sensitivity of the procedure to short-time variations in the system, while the smaller the number of equations, the less discerning the procedure is between noise and signal. The time step used in this example is $\Delta t = 0{\cdot}06$ s and the resolution level is $j = 9$. The abrupt stiffness changes for the s.d.o.f. simulations are given by $k(t) = k_0$ for $t < T/4$, $k(t) = 0{\cdot}75\, k_0$ for $T/4 \leqslant t < 3/8\ T$, $k(t) = 0{\cdot}9\ k_0$ for $3/8\ T \leqslant t < 4.5/8T$, $k(t) = 0{\cdot}75\ k_0$ for $4{\cdot}5/8\ T \leqslant t < 5/8\ T$ and $k(t) = 0{\cdot}9\ k_0$ for $t \geqslant 5/8\ T$. The values of the parameters are $k_0 = 39{\cdot}0$ and $c = 1{\cdot}0$.

As far the 2-d.o.f system, the same abrupt stiffness changes have been assumed for both d.o.f.s. Namely, $k(t) = k_0$ for $t < T/4$, $k(t) = 0{\cdot}75\ k_0$ for $T/4 \leqslant t < T/2$, $k(t) = 0{\cdot}9\ k_0\ t \geqslant T/2$. The values of the parameters are $k_{1,0} = 39{\cdot}0$, $k_{2,0} = 35{\cdot}0$ and $c_1 = 1{\cdot}26$, $c_2 = 1{\cdot}1$.

Least-squares solutions over sequential subsets of 32 equations have provided the estimates shown in Figures 9 and 10.

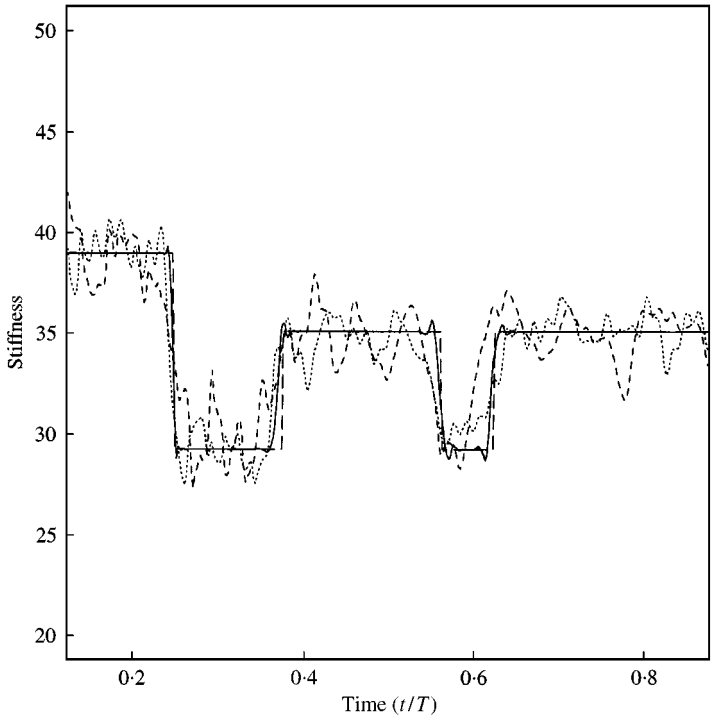

Figure 9. LTV s.d.o.f. system: abrupt varying stiffness estimates; ——, no noise; ····, 5%; - - -, 10%; – – –, true.

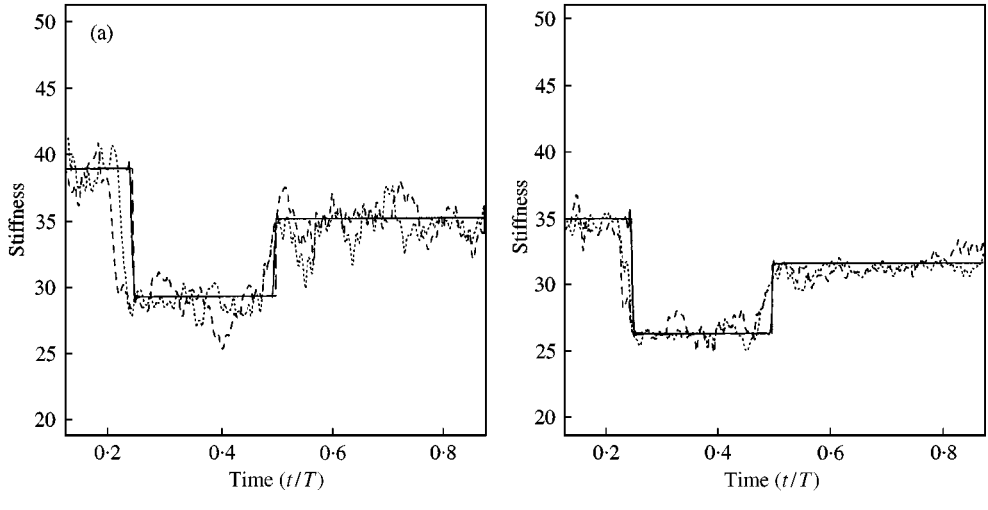

Figure 10. LTV 2-d.o.f. system: abrupt varying stiffness estimates; (a) first element, (b) second element. ——, no noise; ····, 5%; - - -, 10%; – – –, true.

5. CONCLUSIONS

In this paper the wavelet framework has been adopted to describe the evolution of dynamical systems. The Wavelet–Galerkin approach is used to discretize the governing equations. From measurements of input and output data, estimate of the parameters of the

governing differential equation are then obtained. S.d.o.f. and 2-d.o.f. systems undergoing forced and free vibrations have been studied. The damping and stiffness parameters of a linear time-invariant system have been accurately estimated. Moreover, the same identification procedure has been shown to be effective in tracking idealized time evolutions of the unknown parameters. The number of equations entering the least-squares estimates arising from the associated algebraic problem can be interpreted as a design parameter that enables the fine tuning of the algorithm to the particular problem at hand. The analysis and performance of the technique under the realistic conditions of noisy data has also been presented. It has been shown that the presence of noise can affect the accuracy of the predicted evolution of damping estimates while rather robust estimates of the stiffness parameters can be obtained.

REFERENCES

1. C. C. Lin, T. T. Soong and H. G. Natke 1990 *Journal of Engineering Mechanics* **116**, 2258–2274. Real-time system identification of degrading structures.
2. H. Iemura and P. C. Jennings 1974 *Earthquake Engineering and Structural Dynamics* **3**, 183–201. Hysteretic response of a nine-storey reinforced concrete building.
3. F. E. Udwadia and M. D. Trifunac 1974 *Earthquake Engineering and Structural Dynamics* **2**, 359–378. Time and amplitude dependent response of structures.
4. F. E. Udwadia and N. Jerath 1980 *Journal of the Engineering Mechanics Division, Proceedings of the ASCE* **106**, 11–121. Time variations of structural properties during strong ground shaking.
5. W. N. Patten, R. L. Sack and Q. He 1996 *Journal of Structural Engineering* **122**, 187–192. Controller semiactive hydraulic vibration absorber for bridges.
6. K. Liu 1997 *Journal of Sound and Vibration* **206**, 487–505. Identification of linear time-varying systems.
7. A. Al-Khalidy, M. Noori, Z. Hou, R. Carmona, S. Yamamoto, A. Masuda and A. Sone 1997. *Approximate Methods in the Design and Analysis of Pressure Vessels and Piping Components, ASME* PVP-Vol. 347, 49-58. New York: ASME. A study of health monitoring systems of linear structures using wavelet analysis.
8. W. J. Wang and P. D. McFadden 1996 *Journal of Sound and Vibration* **192**, 927–939. Application of wavelets to gearbox vibration signals for fault detection.
9. W. J. Staszewski and R. G. Tomlinson 1994 *Mechanical Systems and Signal Processing* **8**, 289–307. Application of the wavelet transform to fault detection in a spur gear.
10. W. J. Staszewski, C. Biemans, C. Boller and G. R. Tomlinson 1998 *Proceedings of ISMA*23, Vol. I, 59–66. Damage detection using wavelet-based statistical analysis.
11. K. M. Liew and Q. Wang 1998 *Journal of Engineering Mechanics* **124**, 152–157. Application of wavelet theory for crack identification in structures.
12. G. Naldi, and P. Venini 1997 *Meccanica* **32**. Wavelet analysis of structures: statics, dynamics and damage identification.
13. M. Ruzzene, A. Fasana, L. Garibaldi and B. Piombo 1997 *Mechanical Systems and Signal Processing* **11**, 207–218. Natural frequencies and dampings identification using wavelet transform: application to real data.
14. A. N. Robertson, K. C. Park and K. F. Alvin 1998 *Journal of Vibration and Acoustics, Transaction of ASME* **120**, 252–260. Extraction of impulse response data via wavelet transform for structural system identification.
15. R. Glowinski, W. M. Lawton M. Ravachol and E. Tenenbaum 1990 *Computing Methods in Applied Science and Engineering*. 55–120, chapter 4. Wavelet solution of linear and nonlinear elliptic, parabolic and hyperbolic problems in one space dimension.
16. K. Amaratunga, J. R. Williams, S. Qian and J. Weiss 1994 *International Journal for Numerical methods in Engineering* **37**, 2703–2716. Wavelet–Galerkin solutions for one dimensional partial differential equations.
17. I. Daubechies, 1988 *Communications in Pure and Applied Mathematics* **41**, 909–996. Orthonormal bases of compactly supported wavelets.
18. A. Latto, H. Resnikoff and E. Tenenbaum 1992 *Proceedings of the French–USA. Workshop on Wavelets and Turbulence, Princeton University*, June, New York: Springer. The evaluation of connection coefficients of compactly supported wavelets.

19. M. Q. CHEN, C. HWANG and Y. P. SHIH 1996 *International Journal for Numerical methods in Engineering*, **39**, 2921–2944. The computation of Wavelet-Galerkin approximation on a bounded interval.
20. R. GHANEM and F. ROMEO 1998 *Proceedings of the* 16*th IMAC*, 2–6 February, Santa Barbara. Identification of dynamical systems in the wavelet domain.
21. D. L. DONOHO and I. JOHNSTONE 1992 *Technical Report no*. 400, *Department of Statistics*, *Stanford University*. Ideal spatial adaptation via wavelet shrinkage.
22. S. MALLAT, and W. L. HWANG 1992 *IEEE Transactions on Information Theory* **38**, 617–643. Singularity detection and processing with wavelets.
23. S. MALLAT and S. ZHONG 1992 *IEEE Transactions on Pattern Analysis and Machine Intelligence* **14**, 710–732. Characterization of signals from multiscale edges.